I.J. Image, Graphics and Signal Processing, **2023, 6, 28-40**
Published Online on December 8, 2023 by MECS Press (http://www.mecs-press.org/)
DOI: 10.5815/ijigsp.2023.06.03

Enhancement of Mammographic Images Based on Wavelet Denoise and Morphological Contrast Enhancement

Toan Le Van*
Department of Physics and Computer Science, University of Science, Vietnam National University, Ho Chi Minh City, Vietnam
Email: toanlevan1296@gmail.com
ORCID ID: https://orcid.org/0009-0001-0342-7734
*Corresponding Author

Liet Van Dang
Department of Physics and Computer Science, University of Science, Vietnam National University, Ho Chi Minh City, Vietnam
Email: dangvanliet@gmail.com
ORCID ID: https://orcid.org/0009-0008-0795-8891

Received: 07 March, 2023; Revised: 09 April, 2023; Accepted: 22 May, 2023; Published: 08 December, 2023

Abstract: Breast cancer can be detected by mammograms, but not all of them are of high enough quality to be diagnosed by physicians or radiologists. Therefore, denoising and contrast enhancement in the image are issues that need to be addressed. There are numerous techniques to reduce noise and enhance contrast; the most popular of which incorporate spatial filters and histogram equalization. However, these techniques occasionally result in image blurring, particularly around the edges. The purpose of this article is to propose a technique that uses wavelet denoising in conjunction with top-hat and bottom-hat morphological transforms in the wavelet domain to reduce noise and image quality without distorting the image. Use five wavelet functions to test the proposed method: Haar, Daubechies (db3), Coiflet (coif3), Symlet (sym3), and Biorthogonal (bior1.3); each wavelet function employs levels 1 through 4 with four types of wavelet shrinkage: Bayer, Visu, SURE, and Normal. Three flat structuring elements in the shapes of a disk, a square, and a diamond with sizes 2, 5, 10, 15, 20, and 30 are utilized for top-hat and bottom-hat morphological transforms. To determine optimal parameters, the proposed method is applied to mdb001 mammogram (mini MIAS database) contaminated with Gaussian noise with SD, $\sigma = 20$. Based on the quality assessment quantities, the Symlet wavelet (sym3) at level 3, with Visu shrinkage and diamond structuring element size 5 produced the best results (MSE = 50.020, PSNR = 31.140, SSIM = 0.407, and SC = 1.008). The results demonstrate the efficacy of the proposed method.

Index Terms: Breast cancer, Discrete Wavelet Transform, mammogram, denoising, wavelet shrinkage, top-hat, bottom-hat.

1. Introduction

According to GLOBOCAN 2020 [1], breast cancer is the second leading cause of cancer death in women after lung cancer. Each year, more than 2.2 million people worldwide are diagnosed with the disease and 680,000 people die from breast cancer. Experts confirm that breast cancer is 100% curable if it is detected early and treated properly. Early detection of the disease helps us to act proactively and conveniently, to intervene effectively, and to save costs. Mammography is a highly effective and reliable method of detecting and diagnosing breast cancer because it can detect small changes in breast tissue that may indicate the presence of a lump or tumor that may not be visible on a physical examination. However, mammograms are naturally noisy and frequently have areas of low contrast. In addition, because dense (fibrous and glandular) breast tissue, breast mass, and cancer are all relatively bright, it can be challenging to detect tumors.

To reduce noise and improve contrast in mammography, many techniques have been proposed, including Discrete Wavelet Transform (DWT) [2]. This technique is widely employed in image processing, including image compression, denoising, and pattern recognition. In mammography images, wavelet shrinkage was used in combination with the median filter to remove additive and multiplicative noise [3].

The challenges in this topic are noise reduction without blurring image details (edges) and enhancing local details in low-contrast regions. In this paper, we present a method for reducing noise and improving contrast in mammography images by combining wavelet shrinkage with morphological operations (top-hat and bottom-hat transforms) in the wavelet domain to avoid the drawbacks indicated above. Wavelet denoising is based on the choice of wavelet function, decomposition level and the threshold type (shrinkage); the morphological operation is based on the choice of shape and size of structuring element. The method was examined using quality metrics such as Mean Square Error (MSE), Peak Signal-to-Noise Ratio (PSNR), Structural Content (SC), Structural Similarity Index (SSIM) and compared to other methods using a mammography image contaminated with Gaussian noise.

The remainder of the paper is organized as follows: Section 2 gives an overview of related literature. Section 3 describes the proposed method. Section 4 presents the results and discussion and finally is conclusion.

2. Literature Review

In image processing, noise refers to any unwanted variation or distortion in an image that affects its quality and makes it difficult to analyze, process, or interpret. Gaussian noise is inherent in mammograms, even with standard equipment and careful handling. Wiener filters, Gaussian filters or median filters are commonly used to reduce the influence of errors and noise on the mammogram, thereby improving image processing and disease diagnosis ability. As shown above, after filtering, the image is blurry in some cases, especially around the edges. To solve the problem, wavelet shrinkage was used.

In the literature, many different wavelet shrink techniques such as Visu and Bayer have shown better efficiency in image denoising. In addition, much work has been done in the past to reduce noise and improve contrast in medical images. Scharcanski et al. [4] developed an adaptive method based on wavelet transform to reduce noise and enhance medical image; with this method, the image is first pre-processed to increase local contrast and fine detail. Then the image is processed into the wavelet domain to reduce noise and edge enhancement. Han et al. [5] proposed an enhancement threshold method based on wavelet analysis; with this method, different thresholds are chosen for each difference signal frequency to eliminate noise where performance is better achieved. Qian et al. [6] proposed a novel hybrid method based on adaptive averaging filtering and wavelet shrinkage; with this method, more image details and edge information can be preserved. There are many methods are for denoising for medical images based on wavelet shrinkage [2].

This article is about noise reduction using wavelet shrinkage. This can be seen as a continuation of the work listed above. In addition, contrast enhancement through morphological operations (especially top-hat and bottom-hat transforms) and their conjugation with wavelet denoising in the wavelet domain is a new proposal.

3. The Proposed Method

The proposed algorithm is depicted in Figure 1. The mini-MIAS (Mammographic Image Analysis Association) database [7] was used to acquire mammography data, which contains 330 digital mammograms (including 207 normal, 69 benign, and 54 malignant) digitized films from the UK National Breast Screening Program. The images were stored in .pgm format with a resolution of 1024 x 1024 and 8 bits per pixel. Despite the fact that there is a disparity between normal and abnormal mammograms, this not only has a negative influence on mammogram classification but also has

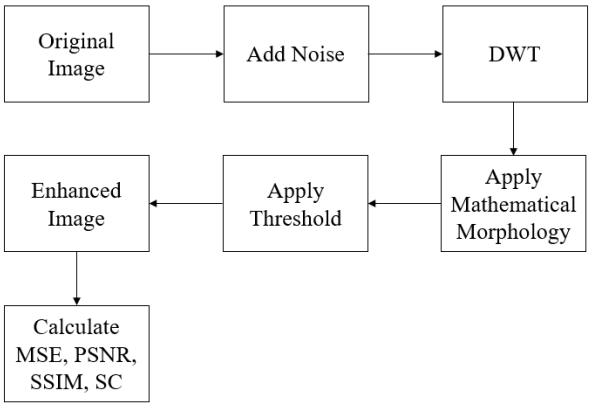

Fig. 1. The basic steps of the proposed algorithm

no effect on image enhancement or tumor detection. Because each image provides the density of breast tissue as well as the type and location of abnormalities, the mini-MIAS database is commonly used in mammography articles. The MIAS mdb001 image was used in the experimental computations in this article, and the results are presented in Tables 3 through Table 7.

3.1 Discrete Wavelet Transform

3.1.1 1D and 2D Discrete Wavelet Transform

The Discrete Wavelet Transform (DWT) is a mathematical technique used to decompose a signal into a set of wavelet coefficients with different scales and positions. In image processing, the DWT is often used to decompose an image into a series of coefficients that can be used to represent the image in a more efficient and compact form. The Discrete Wavelet Transform is a multi-resolution transform with a tree-structured discrete filter bank with two-stage decomposition and reconstruction. In the decomposition stage, the original signal is first filtered through low-pass filter (generated by the scaling function) and a high-pass filter (generated by the wavelet function) to produce low-pass and high-pass sub-bands. The low-pass sub-band is then repeatedly filtered using the identical scheme described above to produce narrower high-pass and low-pass sub-bands. In each successive sub-band, the output is downsampled to ensure that the number of calculations does not increase. In the reconstruction stage, the upsampling results after the decompositions can be synthesized by an inverse wavelet transform to reconstruct the original signal. A two-level 1D DWT decomposition and reconstruction is shown in Fig. 2.

Due to the separability of two-dimensional wavelet filters, a 2D-DWT can be generated from a 1D-DWT, as shown below. First, using 1D-DWT, create L and H sub-bands in each row of the original image. Next, perform a 1D-DWT on each column to obtain four level 1 sub-bands LL1, LH1, HL1 and HH1. Iterating the same scheme for sub-band LL1 leads to LL2, LH2, HL2, and HH2,… Fig. 3 shows the level 1 of the 2D DWT decomposition [8].

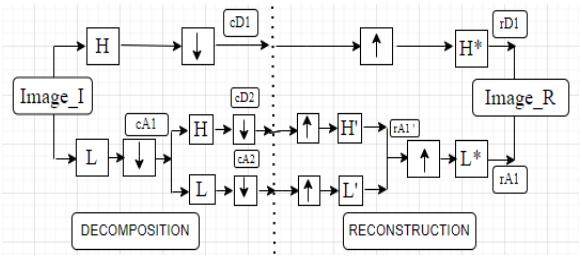

Fig.2. First level 1D-DWT L, H: Decomposition low-pass and high-pass filter L*, H*: Reconstruction low-pass and high-pass
↑: upsampling, ↓: downsampling

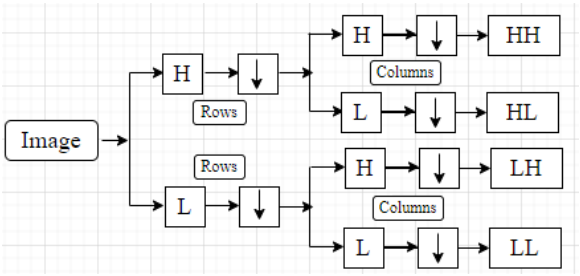

Fig.3. First levels of decomposition in 2D-DWT, L: low-pass filter , H: high-pass filter
↓: downsampling

3.1.2. Wavelet Denoising

In 2D-DWT, each level has four sub-bands; the LL sub-band, known as the approximation component, shows a general trend in pixel values; the other components, called detail components, contain high frequencies including noise; HL for the horizontal detail component, LH for the vertical detail component, and HH for the diagonal detail component. As a result, noise is included in the detail components, especially the HH component. Therefore, threshold is used to perform noise reduction on the detailed components, and an inverse wavelet transform can lead to a less noisy reconstruction. Table 1 summarizes the most often used types of threshold wavelet shrinkage in wavelet denoising [9, 10].

Table 1. Types of threshold [6]

SHRINK	FORMULA		EXPLANATION
VisuShrink	$T=\sigma\sqrt{2\log N}$	(1)	σ^2 is the noise variance (Eq. 1) and N is the number of pixels in the image. This is a practical threshold that effective decreases additive noise (Gaussian noise), $Y_{ij} \in$ HH sub-band
	$\sigma^2=\left[\frac{median\left(\lvert Y_{ij}\rvert\right)}{0.6745}\right]^2$	(2)	
SURE Shrink	$T=\min(t,\sigma\sqrt{2\log n})$	(3)	t: the value that minimizes Stein's Unbiased Risk Estimator, σ^2: the variance of noise(Eq. 1), n: the size of the image.
Bayes Shrink	$T=\frac{\sigma^2}{\sigma_s}$	(4)	σ^2 is the noise variance (Eq. 1), σ: the signal without noise standard deviation. In addition noise, w ϵ HH: $\sigma_w^2=\sum_{x,y=1}^{n} w^2(x,y)/n^2$
	$\sigma_w=\sigma_s+\sigma$	(5)	
	$\sigma_s=\sqrt{\max(\sigma_w^2-\sigma^2,0)}$	(6)	Using Bayes Shrink threshold is smoother than using SURE Shrink threshold
Normal Shrink	$\beta=\sqrt{\log\left(\frac{L_j}{M}\right)}$	(7)	σ^2: the variance of the noise (Eq. 1), σ_y: the standard deviation of the sub-band , β: the scale parameter, L_j: the length of the sub-band at level j, M:total number of decomposition.
	$T=\beta\frac{\sigma^2}{\sigma_y}$	(8)	

Wavelet denoising is the common approach in medical imaging. However, the result is only accepted if the associated quantities such as wavelet function, level decomposition, and wavelet shrinkage are appropriate. This article, five wavelet functions are tested: Haar wavelet (harr), Daubechies wavelet (db4), Coiflet wavelet (coif2), Symlet wavelet (sym3), and Biorthogonal wavelet (bioir 1.3), which belong to different wavelet families. In each function, four types of wavelet shrinkages, namely Visu, SURE, Bayes and Normal are used in each level decomposition (from level 1 to level 4) to discover an acceptable wavelet function, level decomposition and shrinkage type for mammography noise reduction. Section 4 explains how these quantities were chosen.

3.2. Morphological contrast enhancement

Contrast Limited Adaptive Histogram Equalization (CLAHE) is one of the most commonly used contrast enhancement methods. It does this by clipping redistributing the histogram, so that there is no one-to-one relationship between the gray levels of the input and output images. This technique is therefore unsuitable for contrast enhancement in tumor detection because it produces artifacts at high-intensity gradients (at the edges of the object). To overcome the shortcomings of the CLAHE method, the proposed method employs a combination of top-hat and bottom-hat morphological transforms for contrast enhancement.

Morphology is a broad range of image processing methods that process images depending on their shape. Based on a structuring element, each image pixel corresponds in a morphological operation to the value of another pixel in its neighbourhood [11]. There are four basic morphological operations: dilation, erosion, opening and closing. Each morphological operator can be considered as a filter to expand or shrink as well as eliminate or fill the object boundary based on the shape and size of the structural element. The two image enhancement transforms are:

- The top-hat transform returns small objects that are brighter than their surroundings and smaller than the structural element:

$$M_{TH}(i,j) = OI(i,j) - (OI \circ SE)(i,j) \tag{9}$$

- The bottom – hat transform returns objects that are darker than their surroundings and smaller than the structural element:

$$M_{BT}(i,j) = OI(i,j) - (OI \bullet SE)(i,j) \tag{10}$$

where: OI denotes the original image, SE denotes the structural element, ° denotes the Morphological Opening Operation, and • denotes the Morphological Closing Operation.

The image is enhanced by adding the top-hat transform (the bright areas) and subtracting the bottom-hat transform (the dark areas), given by equation:

$$M_{EN} = M + M_{TH} - M_{BH} \tag{11}$$

Equation (11) is called Dual morphological enhancement [12].

In this article, the *modified morphological contrast enhancement* is calculated for each detail component (HL, LH, and HH) after using the 2D-DWT to denoise the image. In Eq. (9) and Eq. (10), *OI* is replaced by a *blurred image* by weighted average filtering, and in Eq. (11), *OI* is replaced by its *high-pass values* (the original image subtract background); this selection is for further contrast improvement and does not require any preprocessing. In the morphological operations, the structuring element, an important neighborhood-defining matrix used in pixel-by-pixel processing, has a significant impact on the results; it must be chosen to match the shape and size of the objects in the input image (tumors in the mammogram). This issue is addressed in Section 4.2.

3.3 Image quality metric

The following quantities in Table 2 are used to compare the quality of the image enhancement to the original reference image [13].

Table 2. Image quality metrics [13]

QUALITY METRIC	FORMULA	EXPLANATION
Mean square Error (MSE)	$\frac{1}{MN}\sum_{i=1}^{M}\sum_{j=1}^{N}(\hat{f}(i,j)-f(i,j))^2$ (12)	MSE indicates the approximate level between the original image and the processed image. The result is better when MSE is smaller.
Peak Signal to Noise Ratio (PSNR)	$10.\log_{10}\frac{Max_I^2}{MSE}$ (13) *Max_i = 255 for 8 bits per sample image*	The PSNR is the ratio between the maximum original signal power and the noisy signal power and is expressed as a logarithmic scale (dB). The result is better when PSNR is larger.
Structural Content (SC)	$\frac{\sum_{i=1}^{M}\sum_{j=1}^{N}(f(i,j)^2}{\sum_{i=1}^{M}\sum_{j=1}^{N}(\hat{f}(i,j))^2}$ (14)	SC is the ratio of the sum of squares of the original image pixels to the sum of squares of the processed image pixels. The best value of SC is equal to 1 (higher value specifies poor the quality)
Structural Similarity Index (SSIM)	$\frac{(2\mu_f\mu_{\hat{f}}+C_1).(2\sigma_{f.\hat{f}}+C_2)}{(\mu_f^2+\mu_{\hat{f}}^2+C_1).(\sigma_f^2+\sigma_{\hat{f}}^2+C_2)}$ (15) μ_f is the mean over a window in input image $\mu_{\hat{f}}$ is the mean over a window in output image σ_f is standard deviation over a window in output image $\sigma_{\hat{f}}$ is standard deviation over a window in output image $\sigma_{f\hat{f}}$ is co-variance over a window between input and output images ; C_1, C_2 are constants.	SSIM measures the difference in perception between two images using visible structures. It is the correlation of two signals based on luminance (mean intensity), contrast (standard deviation) and structural (correlation between two images). Its value should be large for better results.

Table 2 contains the formulas for measuring the quality of the de-noised images; these formulas evaluate distortions between the de-noised image and the reference image. MSE (Eq. (12)) is a simple quality metric that measures the amount of error between original and enhancement images by evaluating the mean squared difference between original and reconstruction values. If the enhanced and original images match, the MSE should be zero. However, when using mean square error, an outlier also affects the MSE value, and is highly dependent on the image intensity scale (number of bits used to represent the intensity of each pixel). Therefore, the PSNR, the ratio between the maximum power of the original image and the processed image in decibels (logarithmic scale), is used to address this deficiency. Eq. (13) gives the PSNR; where, Max_i is the maximum value of the gray level contained in the image. If the gray level is in b-bit, then $Max_i = 2^b - 1$ (for 8-bit image, $Max_i = 2^8 - 1 = 255$). PSNR is regarded as a close approximation of human perception image quality and is thus frequently used to assess the quality of processed images. Because PSNR is inversely related to MSE, the higher the PSNR, the better the image quality. When assessing image quality, the two methods MSE and PSNR are widely used due to their simple calculation, long history and clear physical meaning. However, the disadvantage of PSNR is that it uses the maximum value of the image intensity scale and not the actual intensity of the image. Therefore, numerous alternative quality criteria for determining image quality have been developed.

SC (Eq. (14)) as a method for dealing with the spatial arrangement of pixels in an image. It is used to assess the similarity of two images when the human eye cannot distinguish. The SC value is equal to 1 if two images are identical; the worse the image quality, the higher the SC value. SSIM (Eq. (15)), which is a function of luminance, contrast, and structural terms, is a superior quality measure. Luminance (means intensity) makes the distorted parts of the image appear less clear at the edges. Contrast (standard deviation) makes distortions in the texture of an image less visible. Structural information (correlation) relates to some more important information about the objects visible in the image. These are the quantities that represent the perception conveyed by SSIM that is large to get better results. This metric is commonly used in mammography diagnosis and tumor detection [14].

4. Results and Discussion

As mentioned in the introduction, the objective of the study is to improve image quality by wavelet denoising and contrast enhancement by morphology in the wavelet domain. Therefore, the experimental part is divided into two stages: the first consists in the selection of the parameters for wavelet denoising, the second in the selection of the shape and size of the structure element for morphological contrast enhancement.

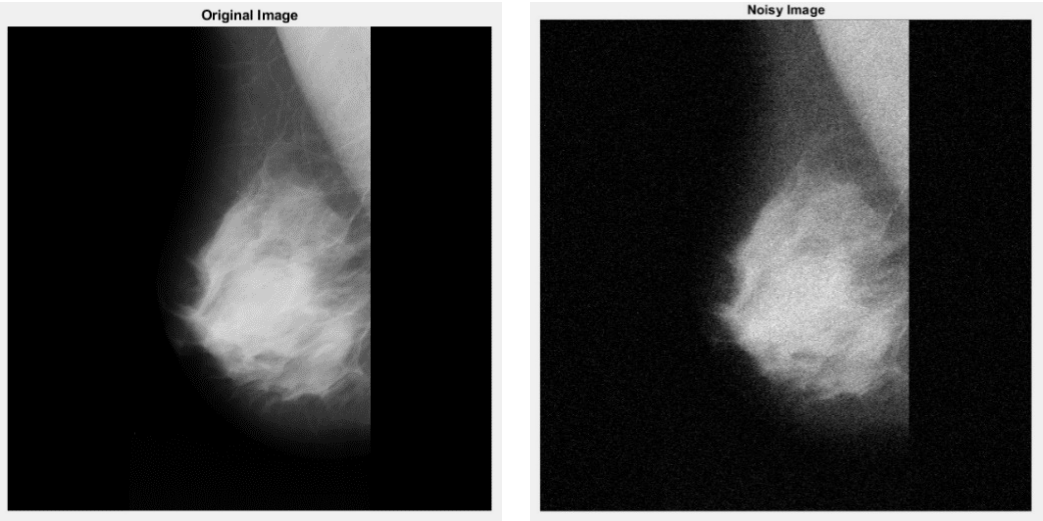

(a) (b)

Fig.4. (a) Input Images (mdb001) and (b) Noisy image mdb001 (Gaussian Noise, $\sigma = 20$), MSE = 256.5375, PSNR = 24.0393

Matlab software is used to model experiments to study these stages. The source image is an mdb001 image from the Mini-MIAS database [7] (Fig. 4a) that has Gaussian noise contaminated with $\sigma = 20$ (Fig. 4b) and is referred to as the noisy image mdb001, as input to the wavelet denoising. This setting was chosen because it is an instinctive noise of the mammogram. Therefore, using a Gaussian noise image to assess noise reduction is more realistic than other forms of noise. The reference image to assess image quality is the original image.

4.1. Selection of parameters for wavelet denoising

Wavelet denoising employs two thresholding techniques: hard thresholding and soft thresholding. However, since the results of the two thresholds are equivalent, the experimental results of our calculations are hard-threshold.

This section discusses how to choose parameters for wavelet denoising, such as the wavelet function, level decomposition, and wavelet shrinkage (threshold). Orthogonal wavelets (including haar, db3, coif2, sym3) and biorthogonal wavelets (bior1.3) are used. The 2D-DWT computes for each wavelet function from level 1 to level 4 using the noisy image mdb001 (Fig. 4b) as input. At each level, each detail component (LH, HL, and DD) is treated as follows: First, one of the four wavelet shrinkages (Visu, Bayer, SURE, and Normal) is selected. Second, contrast enhancement is calculated using a dual morphological enhancement with a structuring element of disk size 10. A hard-threshold is then used to denoise the contrast enhancement output. Finally, the output image is generated by the inverse discrete wavelet transform for noise reduction and contrast enhancement (image enhancement). Quality is assessed using the metric criteria listed in Table 1.

Table 3 though Table 7 show the quality of image denoising with five wavelet functions using Mean Square Error (MSE), Peak Signal-to-Noise Ratio (PSNR), Structure Similarity Indexing (SSIM) and Structure Content (SC). The best denoised image has the lowest MSE, highest PSNR and SSIM and SC is close to one.

Table 3 displays the results of the image denoising quality assessment using the Haar wavelet. Haar is a compact support discrete wavelet that uses a square wave as the first wavelet function. A comparison of the image denoising quality using the Haar wavelet function shows that level 3 wavelet decomposition with Visu shrinkage gives the best

result (MSE = 52.9202, PSNR = 30.8946, SSIM = 0.3701 and SC = 1.0104) and at level 4 with Sure shrinkage gives the worst result (MSE = 561.4287, PSNR = 20.6379, SSIM = 0.0522 and SC = 1.1130).

Table 4 displays the results of the Daubechies (db3) image denoising quality evaluation, which are comparable to Table 3. Daubechies (db from 2^{nd} to 10^{th} order) is the most common family of orthogonal wavelets with asymmetric shape and compact support. The quality assessment result of db3 image denosing at level 3 with Visu shrinkage (Table 4) gives the best result (MSE = 52.6385, PSNR = 30.6047, SSIM = 0.3436, and SC = 1.0195) and at level 4 with Sure shrinkage gives the worst result (MSE = 549.3210, PSNR = 20.7325, SSIM = 0.0532, and SC = 1.0826).

The quality metric results of image denoising with the Coiflet (coif2) and Symlet (sym3) functions are shown in Tables 5 and 6. Both functions belong to the orthogonal wavelet family, are quite symmetric, and compact support. However, the filter length of Cofflet is 6N (N: order of the wavelet function) while the filter length of Symlet is 2N. According to the results in Tables 5, the best image denoising using Coiflet wavelet at level 3 decomposition with Visu shrinkage gives the best result (MSE = 52.2146, PSNR = 30.9529, SSIM = 0.3866, SC = 1.0106) and at level 4 with Sure shrinkage gives the worst result (MSE = 551.0158, PSNR = 20.7192, SSIM = 0.0528, and SC = 1.1095). Tables 6 shows the noise reduction rating with Symlet wavelet. The result shows that decomposition at level 3 with Visu shrinkage gives the best result (MSE = 51.2024, PSNR = 31.0379, SSIM = 0.3859, and SC = 1.0109)) and at level 4 with Sure shrinkage gives the worst result (MSE = 549.4229, PSNR = 20.7317, SSIM = 0.0530, and SC = 1.1077).

Table 7 displays the results of the image denoising quality assessment using the biorthogonal wavelet (bior1.3). The results obtained with the biorthogonal function are similar to those obtained with orthogonal functions. The noise reduction achieved with Visu shrinkage at level 3 gives the best result (MSE = 54.6555, PSNR = 30.7545, SSIM = 0.3645 and SC = 1.0116), while the result with Sure shrinkage at level 4 gives the worst result (MSE = 562.3391, PSNR = 20.6308, SSIM = 0.0513, and SC = 1.1072).

Table 3. The values of image quality metrics MSE, PSNR, SSIM and SC of the wavelet denoising (the noisy image mdb001, Gaussian noise, $\sigma = 20$) using Haar wavelet (haar)

	Level 1				Level 2			
SHRINK	MSE	PSNR	SSIM	SC	MSE	PSNR	SSIM	SC
Bayer	197.2417	25.1808	0.1374	1.0398	188.4581	25.3787	0.1434	1.0383
Visu	99.7624	28.1411	0.2367	1.0209	60.9047	30.2843	0.3443	1.0130
SURE	478.4786	21.3322	0.0581	1.0926	532.7923	20.8652	0.0527	1.1037
Normal	375.6093	22.3834	0.0758	1.0737	406.5126	22.0401	0.0706	1.0793
	Level 3				Level 4			
SHRINK	MSE	PSNR	SSIM	SC	MSE	PSNR	SSIM	SC
Bayer	191.0136	25.3202	0.1420	1.0393	198.6853	25.1491	0.1417	1.0436
Visu	52.9202	30.8946	0.3701	1.0104	53.8320	30.8204	0.3670	1.0111
SURE	548.9871	20.7352	0.0525	1.1073	561.4287	20.6379	0.0522	1.1130
Normal	419.5152	21.9033	0.0690	1.0829	425.1071	21.8458	0.0699	1.0869

Table 4. The values of image quality metrics MSE, PSNR, SSIM and SC of the wavelet denoising (the noisy image mdb001, Gaussian noise, $\sigma = 20$) using Daubechies wavelet (db3)

	Level 1				Level 2			
SHRINK	MSE	PSNR	SSIM	SC	MSE	PSNR	SSIM	SC
Bayer	171.4769	25.7887	0.1527	1.0337	165.4666	25.9437	0.1595	1.0326
Visu	97.8101	28.2270	0.2411	1.0194	59.1577	30.4107	0.3584	1.0118
SURE	475.2442	21.3616	0.0578	1.0911	529.4746	20.8924	0.0522	1.1011
Normal	416.0946	21.9389	0.0704	1.0832	403.3369	22.0741	0.0696	1.0773
	Level 3				Level 4			
SHRINK	MSE	PSNR	SSIM	SC	MSE	PSNR	SSIM	SC
Bayer	162.3993	26.0250	0.1619	1.0339	168.0110	25.8774	0.1618	1.0357
Visu	52.6385	30.6047	0.3436	1.0195	52.0597	30.9658	0.3858	1.0104
SURE	545.0340	20.7666	0.0521	1.1055	549.3210	20.7325	0.0532	1.1078
Normal	412.4834	21.9767	0.0692	1.0809	415.7219	21.9428	0.0706	1.0826

Table 5. The values of image quality metrics MSE, PSNR, SSIM and SC of the wavelet denoising (the noisy image mdb001, Gaussian noise, σ = 20) using Coiflet wavelet (coif2)

	Level 1				Level 2			
SHRINK	MSE	PSNR	SSIM	SC	MSE	PSNR	SSIM	SC
Bayer	177.2834	25.6441	0.1492	1.0345	160.2300	26.0834	0.1635	1.0312
Visu	98.3901	28.2013	0.2408	1.0185	60.0919	30.3426	0.3584	1.0117
SURE	475.7192	21.3573	0.0578	1.0915	530.9193	20.8805	0.0518	1.1017
Normal	374.9168	22.3915	0.0749	1.0717	404.0086	22.0669	0.0694	1.0773
	Level 3				Level 4			
SHRINK	MSE	PSNR	SSIM	SC	MSE	PSNR	SSIM	SC
Bayer	172.9520	25.7515	0.1556	1.0352	173.4874	25.7381	0.1601	1.0377
Visu	52.2146	30.9529	0.3866	1.0106	51.8421	30.9840	0.3854	1.0111
SURE	545.3205	20.7643	0.0520	1.1053	551.0158	20.7192	0.0528	1.1095
Normal	415.4256	21.9459	0.0687	1.0817	417.6247	21.9229	0.0700	1.0842

Table 6. The values of image quality metrics MSE, PSNR, SSIM and SC of the wavelet denoising (the noisy image mdb001, Gaussian noise, σ = 20) using Symlet wavelet (sym3)

	Level 1				Level 2			
SHRINK	MSE	PSNR	SSIM	SC	MSE	PSNR	SSIM	SC
Bayer	173.3111	25.7425	0.1520	1.0335	165.0596	25.9544	0.1594	1.0317
Visu	97.4908	28.2412	0.2422	1.0188	59.2842	30.4014	0.3580	1.0115
SURE	475.3203	21.3609	0.0577	1.0896	530.8064	20.8814	0.0520	1.1011
Normal	371.9037	22.4265	0.0754	1.0711	405.0245	22.0560	0.0693	1.0777
	Level 3				Level 4			
SHRINK	MSE	PSNR	SSIM	SC	MSE	PSNR	SSIM	SC
Bayer	167.5690	25.8889	0.1581	1.0350	167.6566	25.8866	0.1616	1.0356
Visu	51.2024	31.0379	0.3859	1.0109	52.1506	30.9582	0.3849	1.0115
SURE	542.4657	20.7871	0.0521	1.1058	549.4229	20.7317	0.0530	1.1077
Normal	413.9556	21.9613	0.0687	1.0806	416.9761	21.9297	0.0700	1.0841

Table 7. The values of image quality metrics MSE, PSNR, SSIM and SC of the wavelet denoising (the noisy image mdb001, Gaussian noise, σ = 20) using Biorthogonal wavelet (bior1.3)

	Level 1				Level 2			
SHRINK	MSE	PSNR	SSIM	SC	MSE	PSNR	SSIM	SC
Bayer	210.5089	24.8981	0.1308	1.0421	206.8976	24.9732	0.1330	1.0410
Visu	101.9729	28.0460	0.2328	1.0195	63.4420	30.1070	0.3376	1.0133
SURE	479.5126	21.3228	0.0573	1.0913	535.8802	20.8401	0.0516	1.1025
Normal	376.5238	22.3729	0.0747	1.0723	409.9990	22.0030	0.0688	1.0785
	Level 3				Level 4			
SHRINK	MSE	PSNR	SSIM	SC	MSE	PSNR	SSIM	SC
Bayer	210.6317	24.8956	0.1315	1.0413	221.4851	24.6774	0.1304	1.0448
Visu	54.6555	30.7545	0.3645	1.0116	56.2947	30.6261	0.3594	1.0097
SURE	551.2052	20.7177	0.0512	1.1045	562.3391	20.6308	0.0513	1.1072
Normal	421.9262	21.8784	0.0676	1.0816	432.2006	21.7739	0.0679	1.0830

The results presented above show that: (a) Level 3 and level 4 gives better results than levels 1 and 2, (b): Symlet and Coiflet wavelets give better results than Daubechies and Haar wavelets, while Biorthogonal wavelet gives the worst results, (c): Visu shrinkage gives better results than Bayer shrinkage and Normal shrinkage, Sure shrinkage gives the worst results.

Table 8. The values of image quality MSE, PSNR, SSIM and SC of the wavelet denoising (the noisy image mdb001, Gaussian noise, σ = 20) at level 3 of five wavelet families

	Symlet wavelet (sym3)				Biorthogonal wavelet (bior1.3)			
SHRINK	MSE	PSNR	SSIM	SC	MSE	PSNR	SSIM	SC
Bayer	167.5690	25.8889	0.1581	1.0350	210.6317	24.8956	0.1315	1.0413
Visu	**51.2024**	**31.0379**	**0.3859**	**1.0109**	54.6555	30.7545	0.3645	1.0116
SURE	542.4657	20.7871	0.0521	1.1058	551.2052	20.7177	0.0512	1.1045
Normal	413.9556	21.9613	0.0687	1.0806	421.9262	21.8784	0.0676	1.0816
	Daubechie wavelet (db3)				Coiflet wavelet (coif2)			
SHRINK	MSE	PSNR	SSIM	SC	MSE	PSNR	SSIM	SC
Bayer	162.3993	26.0250	0.1619	1.0339	172.9520	25.7515	0.1556	1.0352
Visu	52.6385	30.6047	0.3436	1.0195	52.2146	30.9529	0.3866	1.0106
SURE	545.0340	20.7666	0.0521	1.1055	545.3205	20.7643	0.0520	1.1053
Normal	412.4834	21.9767	0.0692	1.0809	415.4256	21.9459	0.0687	1.0817

	Haar wavelet (haar)			
SHRINK	MSE	PSNR	SSIM	SC
Bayer	191.0136	25.3202	0.1420	1.0393
Visu	52.9202	30.8946	0.3701	1.0104
SURE	548.9871	20.7352	0.0525	1.1073
Normal	419.5152	21.9033	0.0690	1.0829

Specifically, the wavelet denoising for Gaussian noise contaminated with mammography images in the **level 3** decomposition of the **Symlet wavelet** (sym3) using **Visu shrinkage** is the **best denoising**, while level four of the biorthogonal wavelet (bior1.3) using Sure shrinkage is the worst denoising. This result can be explained by the fact that the noisy image (σ = 20), which corresponds to a mammography image with low frequencies in the range from 1/8 to 1/4 of the Nyquist frequency, and when it is changed, the level can change. Regarding the wavelet functions used above, there are only two wavelet functions that are orthogonal and have a quite symmetric shape and compact support, namely the Symlet (sym3) with filter length 2N (N is the degree of the function) and the Coiflet (coif2) with the filter length 6N. The Symlet wavelet gives a better result than the Coiflet wavelet result, suggesting that a symmetric orthogonal wavelet function with a short filter length provides better noise reduction than those with a long filter length. Visu shrinkage [15] could be due to a variety of factors, including its mathematical properties, ability to properly balance denoising and detail preservation, and processing efficiency.

The denoising result using the Symlet wavelet and Visu shrinkage is consistent with the denoising findings of Nasser Edinne Benhassine et al. [16]; the comparison is presented in section 4.3. Table 8 provides a summary of level 3 wavelet denoising results for five wavelet functions with four types of wavelet shrinkage.

4.2. Selection of shape and size of structural element for morphological contrast enhancement

The above section informs about the choice of the parameter of wavelet denoising, where morphological operations do not change the shape and size of the structuring element. In this section, the sym3 function at level 3with Visu shrinkage is used to determine the shape and size of the structuring element (SE) as it determines the quality of the contrast enhancement. In mathematical morphological operations, a flat structuring element with a symmetrical shape is usually used. For this reason, the structuring elements in this section are chosen to have the shape of a disk, a square, and a diamond, with sizes of 2, 5, 10, 15, 20 and 30 pixels, in order to correlate with the tumors in the mammography image. These shapes and sizes were studied to find which would enhance contrast the most. The results of selecting this option are shown in Table 9. Table 9 employs the four quality metrics SE, PSNR, SSIM and SC. The analysis results for each SE with different sizes; these values do not depend on much the shape and size of the SE; MSE from 50.020 to 51.971, PSNR from 31.001 to 31.104, SSIM from 0.381 to 0.407, and SC from 1.007 to 1.011. Analysis of the results: disk SE size 2, square SE size 10 and diamond SE size 5 give the best results. However, for the three SE shapes listed above, ***diamond SE size 5 gives the predominant results*** with MSE = 50,020, PSNR = 31,140, SSIM = 0.407, and SC = 1.008. The results show that all SEs have a symmetrical shape, but diamond SE gives the best results, suggesting that this shape can have multiple edges and thus matches the shape of objects in the mammography image.

Table 9. The values of image quality MSE, PSNR, SSIM and SC of different shapes and sizes of structural element (the noisy image mdb001, Gaussian noise, σ = 20 and DWT using Symlet wavelet function at level 3)

SE. shape	Size	MSE	PSNR	SSIM	SC	Size	MSE	PSNR	SSIM	SC
Disk	*2*	50.332	31.112	0.407	1.008	*15*	50.518	31.096	0.407	1.008
	5	50.456	31.102	0.407	1.007	*20*	51.533	31.010	0.383	1.010
	10	50.476	31.100	0.407	1.008	*30*	51.907	30.979	0.382	1.011
Square	*2*	50.513	31.097	0.407	1.007	*15*	50.681	31.082	0.407	1.008
	5	50.686	31.082	0.406	1.007	*20*	51.535	31.010	0.385	1.011
	10	50.502	31.098	0.407	1.008	*30*	51.588	31.006	0.383	1.011
Diamond	*2*	50.768	31.075	0.407	1.008	*15*	50.783	31.074	0.407	1.007
	5	50.020	**31.140**	0.407	1.008	*20*	51.537	31.010	0.382	1.011
	10	50.552	31.093	0.407	1.008	*30*	51.971	30.973	0.381	1.011

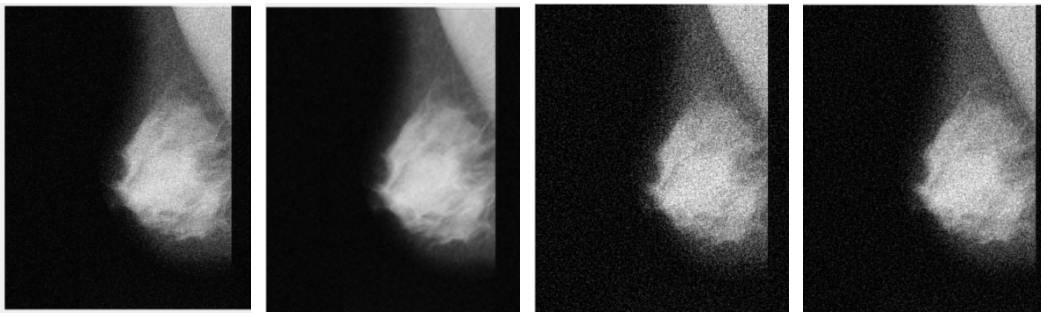

(a) (b) (c) (d)

Fig.5. Image enhancement by proposed method. (a) Bayer (MSE = 147.484, PSNR = 26.443), (b) Visu (MSE = 50.020, PSNR = 31.140), (c) SURE (MSE = 511.699, PSNR = 21.041), (d) Normal (MSE = 380.758, PSNR = 23.243). (Input: noisy image mdb001 (Fig. 4b, Gaussian noise, σ =20, MSE = 256.538, PSNR= 24.039) Processing: Symlet wavelet function (sym3), at level 3, diamond structuring element with r = 5).

Fig. 5 shows the enhanced image of the mdb001 noise image obtained by combining the DWT of the Symlet wavelet function (sym3) at level 3 with the morphological operation using a diamond shape (r = 5) structure element at four different thresholds: Bayes, Visu, SURE, and Normal. The results demonstrate that eliminating Gaussian noise with Visu shrink and enhancing contrast using dual morphological enhancement in the wavelet domain achieves the best image enhancement.

According to the above survey, the main features of the proposed method are: (a): *Choose the wavelet function:* Daubechies wavelets are the most commonly used. However, the results show that the orthogonal wavelet function has a quite symmetrical shape and a short filter length (sym3 function) is appropriate; it is likely that the Daubechies wavelet has an asymmetric shape and is therefore unsuitable for noise reduction in the mammography image; (b): *Wavelet level decomposition:* This is related to the frequency range of the noise contained in the mammography image. The result shows that the level 3 decomposition (1/8 to 1/4 of the Nyquist frequency) is sufficient for Gaussian noise with a standard deviation of 20 in the mammography image; (c): *Size and shape of the morphological structuring element:* The flat structuring element of the disk is used most frequently. However, the results suggest that the size 5 diamond is suitable; it is possible that the diamond has numerous edges that correspond to the shape of the anomalies in the mammography image.

4.3. Comparison of other works

Our proposed method was compared with that of Nasser EdinneBenhassine et al [16]. These authors used the Crow Search Algorithm (CSA) and Social Spider Optimization (SSO) to find the optimal threshold of wavelet coefficients called BLO-DWT-CSA and their results were compared with the Denoising Convolutional Neural Networks (DnCNNs) approach (ref. 51 in [16]). Table 10 shows the results of our proposed method as well as the results of Nasser Edinne Benhassine et al. which contained the results of two techniques, DnCNN and BLO-DWT-CSA. Our results in this table were obtained using the wavelet function and level decomposition, which follows the work of Nasser Edinne Benhassine et al. The results show that our proposed approach achieves lower MSE and higher PSNR values compared to the DnCNN method for all noise SDs of 5, 10, 20, and 30. However, the BLO-DWT-CSA method gives better results

than our results at noise SDs of 5 and 10, but worse at noise SDs of 20 and 30. This result confirms the reliability of our proposed method, particularly when the SD noise is high.

Table 10. MSE and PSNR of proposed method to DnCNN and BLO-DWT-CSA methods. Inputs are mdb001 contaminated by Gaussian noise

σ	Wavelet family	Optimal level	DnCNN [16]		BLO-DWT_CSA [16]		The proposed method	
			MSE	PSNR	MSE	PSNR	MSE	PSNR
5	Sym4	4	8.09	39.05	5.46	40.76	6.92	39.66
10	Sym2	5	43.87	31.71	18.17	35.53	25.20	34.92
20	Sym2	4	181.98	25.53	61.34	30.25	52.61	30.92
30	Sym6	4	396.68	22.15	121.99	27.15	105.75	28.61

Besides adding Gaussian noise to mammograms to evaluate the effect of mammography enhancement, our proposed method was compared with that proposed method by Mohammed N. Qasim et al. [17] and Raagav Ramani et al. [18] using the enhancement of mammograms without adding Gaussian noise. They used the quantum wavelet transform and atrous pyramid convolutional to choose the local thresholds and active contours, which can be utilized to decompose an image into its elements called Quantum wavelet transform filtering. The results of Mohammed N. Qasim et al. were compared with the adaptive fuzzy median filter method and the quantum inverse MFT filtering method (ref. 8 in [17]). And Raagav Ramani et al. used four types of pre-processing filtering: Median filter, Adaptive Median filter, Weiner filter and Mean filter to remove the noise existing in medical images. Of the four filters, Adaptive Median filter has the highest PSNR at 39.8323.

Table 11 shows the results of our proposed method as well as the results of Mohammed N. Qasim et al. which contained the results of two methods: Adaptive fuzzy median filter and Quantum inverse MFT filtering. The results show that our proposed approach achieves higher PSNR values compared to the methods Adaptive fuzzy median filter and Quantum inverse MFT filtering in all windowing size in input image. However, the Quantum wavelet transform filtering gives better results than our results at a 7x7 windowing size in the input image, but worse at the 3x3 and 5x5 sizes.

Table 11. PSNR of proposed method to Quantum wavelet transform filtering, Adaptive fuzzy median filter and Quantum inverse MFT filtering methods. Inputs are mdb004

Noise reduction methods	Windowing size in input image	PSNR
Quantum inverse MFT filtering	3 x 3	35.69
	5 x 5	32.40
	7 x 7	30.78
Noise reduction methods	Windowing size in input image	PSNR
Adaptive fuzzy median filter	3 x 3	33.60
	5 x 5	37.15
	7 x 7	38.39
Quantum wavelet transform filtering	3 x 3	34.57
	5 x 5	38.41
	7 x 7	43.50
The Proposed method	DWT using Symlet wavelet function at level 3, diamond SE size 5	39.90

Table 12 is the results of our proposed method as well as the results of Raagav Ramani et al. Our proposed approach achieves higher PSNR and lower MSE values compared to the four filter types: Median filter, Adaptive Median filter, Weiner filter and Mean filter were used to remove the noise existing in medical images.

Table 12. PSNR, MSE and SC of proposed method to Median filter, Adaptive Median filter, Weiner filter and Mean filter. Input image mdb001

Noise reduction methods	MSE	PSNR	SC
Median filter	14.7559	36.4411	0.9960
Adaptive Median filter	6.7584	39.8323	1.0016
Weiner filter	18.7543	35.3998	0.9969
Mean filter	12.9778	36.9988	1.0056
The Proposed method	2.0792	46.8211	1.0012

The simulation was run on a Matlab platform equipped with a CPU Core i7, 4-core, Intel 2.6 GHz and an 8 GB memory system. For Gaussian noise ($\sigma = 20$), the average execution time for image enhancement (including image denoising and morphological enhancement) is 12.61s for mammogram mdb001 and 12.85s for mammogram mdb004. For a noise-free image, the execution time is 9.38s for mdb001 and 9.59s for mdb004. The above time frame is appropriate for image enhancement with our proposed technique.

5. Conclusion

In this article, a mammography enhancement method based on wavelet shrinkage combined with morphological operations in the wavelet domain is proposed. The novelty aspect of the proposed method is the modification of the dual morphological enhancement step, which avoid the pre-processing by replacing the original image with the smoothed image in the open and closed operations. These two results are added and then subtracted from the high-pass filter image to enhance the contrast at the object boundary. The image enhancement by the proposed method is checked using criteria such as a small MSE, a large PSNR and SSIM index, and SC equal to one. The results show that image enhancement with the sym3 wavelet level 3 using Visu shrinkage and the size 5 flat diamond structuring element gives the best result. With this method, the image enhancement ensures high contrast between the objects and the background and preserves the edges of the image. Unlike traditional methods, the output image is not blurry and free from artifacts, making it suitable for tumor detection. Future work will examine noise reduction through wavelet shrinkage and morphological contrast enhancements applied to mammography images contaminated with a variety of noise, including multiplicative noise, and then use them for tumor detection.

References

[1] https://gco.iarc.fr/today/data/factsheets/populations/704-viet-nam-fact-sheets.pdf.

[2] Vishwanatha, M. C Hanumantharaju, M. T Gopalakrishna, M. Ravishankar, (2013). Mammogram Image Enhancement Techniques for Detecting Breast Cancer: A Critical Review. Proc. of the Second Intl. Conf. on Advances in Electronics, Electrical and Computer Engineering. ISBN: 978-981-07-6935-2 doi:10.3850/ 978-981-07-6935-2_25.

[3] Ms. Dhanushree.V, Mr. M.G.srinivasa (2015). Image Denoising using Median Filter and DWT Adaptive Wavelet Threshold. IOSR Journal of VLSI and Signal Processing (IOSR-JVSP) Volume 5, Issue 3, Ver. I, pp. 50-57.

[4] J. Scharcanski and C. R. Jung (2006). Denoising and enhancing digital mammographic images for visual screening. Computer Medical Imaging and Graphics, vol. 30, no. 4, pp. 243–254, doi: 10.1016/j.compmedimag.

[5] Han M, Liu H, Xi JH, Guo W (2007). Noise smoothing for nonlinear time series using wavelet soft threshold. IEEE Signal Process Lett. Vol:14(1): 62-65, doi:10.1109/LSP.2006.881518.

[6] Qian Y, (2019). Removing of salt-and-pepper noise in images based on adaptive median filtering and improved threshold function. Vol: 1431-1436. Nanchang, China. doi.org/10.1109/ccdc.2019.8832612.

[7] http://www.wiau.man.ac.uk/services/MIAS/MIASweb.html.

[8] https://www.mathworks.com/help/wavelet/gs/continuous-and-discrete-wavelet-transforms.html.

[9] Rajesh Kumar Rai, JyotiAsnani, T. R. Sontakke, (2012). Review of Shrinkage Techniques for Image Denoising. International Journal of Computer Applications (0975 – 8887) Vol. 42– No.19.

[10] SachinRuikar, D.D. Doye, (2010). Image Denoising Using Wavelet Transform. International Conference on Mechanical and Electrical Technology (ICMET 2010). DOI:10.1109/ICMET.2010.5598411

[11] Prateek Chhikara, (2022). Understanding Morphological Image Processing and Its Operations. Towards Data Science.

[12] J. Anitha, J.D. Peter, S.I.A Pandian, (2016). A dual stage adaptive thresholding (DuSAT) for automatic mass detection in mammograms. Computer Methods and Programs in Biomedicine, Vol. 138, pp. 93–104.

[13] Palwinder Singha, Leena Jainb, (2018). Hybridization of Adaptive Wavelet Shrinkage with Guided Filter for Speckle Reduction in Ultrasound Images. Procedia Computer Science, pp. 1718–1727.

[14] S. Rajkumar, G. Malathi, (2016). A Comparative Analysis on Image Quality Assessment for Real Time Satellite Images, Indian Journal of Science and Technology, Vol 9(34., DOI: 10.17485/ijst/2016/v9i34/96766.

[15] Konstantinos N. Plataniotis , Anastasios N. Venetsanopoulos, (2000). Color image processing and applications. Springer-Verlag Berlin Heidelberg. DOI:10.1007/978-3-662-04186-4.

[16] Nasser Edinne Benhassine, Abdelnour Boukaache, Djalil Boudjehem, (2021). Medical image denoising using optimal thresholding of wavelet coefficients with selection of the best decomposition level and mother wavelet. International Journal of Imaging Systems and Technology. Vol. 31, doi:10.1002/ima.22589.

[17] Mohammed N. Qasim, Tareq Abed Mohammed, and Oguz Bayat (2022). Breast Sentinel Lymph Node Cancer Detection from Mammographic Images Based on Quantum Wavelet Transform and an Atrous Pyramid Convolutional Neural Network. Hindawi Scientific Programming. Volume 2022, Article ID 1887613, 13 pages, https://doi.org/10.1155/2022/1887613.

[18] Markos Wondim Walle, Kula Kakeba Tune, Natnael Tilahun Sinshaw, Sudhir Kumar Mohapatra, "Transfer Learning based Breast Cancer Classification via Deep Convolutional Neural Network", International Journal of Engineering and Manufacturing, Vol.13, No.4, pp. 34-43, 2023.

Authors' Profiles

Toan Le Van received the B.S. degree in Physic and Computer Science from the University of Science, Vietnam National University, Ho Chi Minh City, Vietnam in 2018. He is currently pursuing his Master of Engineering Physics from the University of Science, Vietnam National University, Ho Chi Minh City, Vietnam. His area of research interests are Medical Image Processing, Machine/Deep Learning, and Computer Vision.

Liet Van Dang received his Ph.D in Mathematics – Physics from the University of Ho Chi Minh City (now Vietnam National University, Ho Chi Minh City) in 1995. He is an invited Associate Professor at the Dept. Physics – Computer Science at the University of Science (Vietnam National University, Ho Chi Minh City). His areas of interest are Signal and Image Processing, Machine Learning, Gravity and Magnetic data analysis. His email is dangvanliet@gmail.com.

How to cite this paper: Toan Le Van, Liet Van Dang, "Enhancement of Mammographic Images Based on Wavelet Denoise and Morphological Contrast Enhancement", International Journal of Image, Graphics and Signal Processing(IJIGSP), Vol.15, No.6, pp. 28-40, 2023. DOI:10.5815/ijigsp.2023.06.03